NACA

RESEARCH MEMORANDUM

EXPERIMENTAL LIFT OF LOW-ASPECT-RATIO TRIANGULAR WINGS

AT LARGE ANGLES OF ATTACK AND SUPERSONIC SPEEDS

By William A. Hill, Jr.

Ames Aeronautical Laboratory
Moffett Field, Calif.

NATIONAL ADVISORY COMMITTEE
FOR AERONAUTICS

WASHINGTON

November 20, 1957
Declassified April 12, 1961

NATIONAL ADVISORY COMMITTEE FOR AERONAUTICS

RESEARCH MEMORANDUM

EXPERIMENTAL LIFT OF LOW-ASPECT-RATIO TRIANGULAR WINGS

AT LARGE ANGLES OF ATTACK AND SUPERSONIC SPEEDS

By William A. Hill, Jr.

SUMMARY

In order to provide information on the effects of large angles of attack on the lift and normal force on triangular wings in the Mach number range 1.96 to 3.30, three wings of aspect ratio 3/8, 2/3, and 1 were tested at angles of attack up to 47°. The wings had modified biconvex sections in vertical streamwise planes with maximum thickness ratios of 4 percent at the 59-percent chord line and trailing edges blunted to a height one half the maximum thickness.

Near zero angle of attack the normal-force curve slopes were satisfactorily predicted by linear theory. Above angles of attack of about 5°, available nonlinear theories for low-aspect-ratio triangular wings were inadequate for predicting the large nonlinearities in the normal-force curves. Normal-force coefficients could be predicted, however, for angles of attack up to at least 30° by utilizing linear theory plus a nonlinear empirical expression for the nonlinear components of normal-force coefficients.

The data of the present investigation together with data for larger aspect ratio wings from other tests showed that the maximum lift coefficient decreased with increasing Mach number over an aspect ratio range of 3/8 to 4. Effects of aspect ratio became significant only below a value of about 2. The maximum lift coefficient is decreased approximately 30 percent by a decrease in aspect ratio from 2 to 3/8. Maximum lift coefficient could be correlated within ±5 percent when plotted as a function of the ratio of Mach number to aspect ratio.

INTRODUCTION

This report is the sixth in a series on the high-incidence characteristics of wings alone and wings employed as all-movable controls in combination with a body in the Mach number range 1.45 to 3.36. Kaattari

(refs. 1 and 2) measured the pressure distributions on a rectangular wing
of aspect ratio 2 and two triangular wings of aspect ratio 2 and 4. An
analysis of some of the pressure distribution data for the two triangular
wings is presented by Katzen and Pitts in reference 3. In reference 4,
Pitts made a detailed comparison between the experimental and theoretical
loadings on three rectangular wings having aspect ratios 1, 2, and 3.
All of these wings were employed as all-movable controls, as described in
reference 5, by mounting them in combination with a body. The present
report investigates the lift of three triangular wings of aspect ratio
3/8, 2/3, and 1 at angles of attack up to 47°.

SYMBOLS

A	aspect ratio
b	wing span
c	local chord
c_r	root chord
C_L	lift coefficient, $\dfrac{\text{lift}}{q_\infty S}$
$C_{L_{max}}$	maximum lift coefficient
C_N	normal-force coefficient, $\dfrac{\text{normal force}}{q_\infty S}$
$C_{N_{lin}}$	normal-force coefficient from linear theory
M	Mach number
q_∞	free-stream dynamic pressure
r	maximum thickness of filleted root section
S	wing plan-form area
t	local thickness of wing section
α	angle of attack
β	$\sqrt{M^2 - 1}$
ϵ	wing semiapex angle, deg

APPARATUS

The investigation was conducted in the Ames 1- by 3-foot supersonic wind tunnel No. 2. This tunnel is a nonreturn, intermittent-operation, variable-pressure wind tunnel with a Mach number range of 1.4 to 3.8. The Mach number is changed by varying the contour of flexible steel plates which form the upper and lower walls of the nozzle.

The models consisted of three triangular wings of aspect ratios 3/8, 2/3, and 1. A sketch of the models with their dimensions summarized is presented in figure 1. The wings had modified biconvex sections in vertical streamwise planes with maximum thickness ratios of 4 percent at the 59-percent chord line and trailing edges blunted to a height one half of the maximum thickness. All of the wings had filleted root sections to be consistent with tests of similar wings in references 1 through 5. The maximum width of the fillet was 0.1 of the wing span. The maximum height is shown as the dimension r in figure 1. Each wing was supported from the rear by a strut which was attached to a strain-gage balance mounted in the wind tunnel. The front part of each strut was integral with its respective wing. The rear part, which was detachable from the front, was either straight for the angle-of-attack range 0° to $\pm 15^\circ$, or had a 30°-angle bend to increase the available range from $+15^\circ$ to $+45^\circ$, or -15° to -45° (the latter was accomplished by rotating the model 180°). The struts were attached to the wings in either a symmetrical or asymmetrical position, as shown in figure 1. The rear portion of each of the struts, downstream of the wing trailing edge, was shielded from air loads by a shroud.

TEST PROCEDURE

Tests were conducted at Mach numbers of 1.96, 2.43, and 3.30, and at a Reynolds number per inch of 0.85 million. The maximum angle of attack varied between 41° and 47° including deflection of the supports under load. Lift, normal force, drag, and pitching-moment coefficients of each model were measured; however, effects of the model support struts on the drag and pitching-moment coefficients were found to be sufficiently large to warrant exclusion of these data from the present report. It is believed that the struts had only a small effect on lift and normal-force coefficients. An indication of this effect of the struts was obtained from comparisons of lift coefficients of the wing of aspect ratio 3/8 having both symmetrical and asymmetrical struts. These comparisons (fig. 2) show that at low angles of attack the lift measured with the symmetrical strut was identical with the average of the lifts obtained with the asymmetrical strut above and below the wing. At high angles of attack the lift measured with the symmetrical strut was only slightly higher than that obtained with the asymmetrical strut located on the expansion surface. The asymmetrical

strut in this location can contribute at most only a small negative lift, since it is immersed in a flow field of low pressure relative to the undisturbed stream.

PRECISION OF DATA

Uncertainty in the measured values of lift and normal-force coefficients was determined on the basis of repeatability, estimated effects of tunnel-stream asymmetry determined from comparisons of data measured at positive and negative angles of attack, and the uncertainty involved in evaluating the effects of the support strut. The maximum uncertainty in C_L and C_N is estimated to be less than ±0.02. The accuracy in measuring angle of attack is within ±0.1°. The variation in the free-stream Mach number in the region occupied by the models was less than ±0.02 at $M = 1.96$, ±0.03 at $M = 2.43$, and ±0.05 at $M = 3.30$.

RESULTS AND DISCUSSION

Figures 2 to 4 present lift coefficient as a function of angle of attack for each of the wings. In no case was the maximum lift coefficient attained at the maximum angle of attack tested ($\alpha = 47°$). However, an estimate of $C_{L_{max}}$ was obtained by a small extrapolation of each of the lift curves. The extrapolated values of C_L were obtained from a linear extrapolation of corresponding curves of $C_L/\cos \alpha$ vs. α since in the region near maximum lift coefficient $C_L/\cos \alpha$, which is essentially C_N, was approximately linear with α. The extrapolated portions of the lift curves are shown dashed.

Comparisons With Data From Semispan Tests

Prior to the present investigation of full-span triangular wings of low aspect ratio, a similar investigation was conducted which employed semispan triangular wings of small span mounted on a boundary-layer bypass plate. The aspect ratios and sections of the three semispan wings were identical to those of the three wings of the present investigation. Maximum lift coefficients obtained from these semispan tests have been published in reference 6. A subsequent investigation of semispan wings in combination with a half-body (ref. 5), however, has indicated that the lift measured on semispan models of small span is subject to significant effects of interaction of the bypass-plate boundary layer with the model shock wave. Therefore, the present lift data and those obtained from tests of the three semispan models are compared in figure 5 to show the

effects of a boundary-layer bypass plate. It is evident that the lift
curves of the semispan wings are noticeably lower than those of the cor-
responding full-span models throughout the angle-of-attack range, and
particularly near $C_{L_{max}}$. The semispan wing of aspect ratio 3/8, which
experienced the largest effect of the plate, had the smallest semispan
of the three models, 3/4 inch compared to 1-1/2 inches for the aspect
ratio 2/3 and 1 wings. For a wing with a sufficiently large span, the
plate effect on the total lift should be small. For example, references
1 and 2 present the span loadings on two wings of aspect ratio 2 and 4
mounted on the same bypass plate mentioned above. These wings had semi-
spans of 4 inches. Only near $C_{L_{max}}$ do the corresponding span load
distributions of these wings show a slight decrease at the most inboard
station.

Prediction of Lift and Normal Force and Comparison
With Experiment

Several nonlinear theories (refs. 7 through 9) are available for
calculating the lift of low-aspect-ratio triangular wings. These theories,
however, are restricted to wings at subsonic speeds or wings with leading
edges lying well within the Mach cone. The expression for lift is con-
sidered to consist of a linear term for fully attached flow plus a non-
linear viscous term. The viscous term represents the effects of flow
separation from sharp leading edges and the formation of two spiral vor-
tex sheets above the wing surface. Each vortex sheet is approximated by
a concentrated vortex lying inboard of the leading edge. Several differ-
ent theoretical forms of the nonlinear term have arisen. By making some-
what different assumptions as to the details of the flow model and the
boundary conditions involved, Küchemann (ref. 7), Edwards (ref. 8), and
Brown and Michael (ref. 9) develop the following expressions for lift:

$$C_L = C_{L_{lin}} + \frac{\pi^{3/2}}{4} A\alpha^{3/2} \qquad \text{(ref. 7)} \qquad (1)$$

$$C_L = C_{L_{lin}} + \pi A^{1/3} \alpha^{5/3} \qquad \text{(ref. 8)} \qquad (2)$$

$$C_L = C_{L_{lin}} + \pi A^{1/3} \alpha^{5/3} \left[1 + \frac{2}{3} \left(\frac{\alpha}{A} \right)^{2/3} \right] \qquad \text{(ref. 9)} \qquad (3)$$

Equations (2) and (3) were obtained by essentially the same method; how-
ever, equation (3) retains a higher order term. Comparisons of these
equations with the experimental normal-force coefficients are presented
in figure 6. Normal force rather than lift is compared since, for large

angles of attack, equations (1) to (3) actually represent c_N rather
than c_L. It should be noted that for the linear term references 7 to 9
use the result from slender-body theory of $\pi A\alpha/2$ (ref. 10) whereas in
figure 6 the more exact linear-theory value (ref. 11) of $(\pi A\alpha/2)[1/E(k)]$
is used. The function $E(k)$ is the normalized complete elliptic integral
of the second kind of modulus $k = \sqrt{1-\beta^2\tan^2\epsilon}$. Near $\alpha = 0$ the normal-
force curve slopes are approximately those given by linear theory. At
larger angles of attack the divergence of normal-force coefficients calcu-
lated by the various nonlinear methods is apparent. These comparisons
also reflect the opposing trends of the theories and experiment. The non-
linear theories predict an increase in the nonlinear normal-force increment
with increasing aspect ratio, while experiment shows that at a constant
Mach number the normal-force increment (obtained as the difference between
experimental normal-force coefficient and the corresponding linear-theory
value) decreases markedly with increasing aspect ratio. Reference 12
shows this same trend of experiment at low subsonic speeds. Effects of
Mach number are not considered by the various theories; however, the
experimental data show a significant decrease in the normal-force increment
with increasing Mach number.

These effects of Mach number and aspect ratio on the experimental
normal-force increment are shown in figure 7 to correlate with the
parameter $\beta \tan \epsilon$. For angles of attack up to at least 30°, $c_N - c_{N_{lin}}$
is, in general, dependent only on $\beta \tan \epsilon$ and α. As shown in figure 7
this relationship can be approximated by the empirical expression,

$$c_N - c_{N_{lin}} = \frac{\alpha^{3/2}}{4(\beta \tan \epsilon)^{3/4}} \tag{4}$$

for the range $0.15 < \beta \tan \epsilon < 0.8$. The exponent of α in equation (4)
is seen to be identical to that given by Küchemann's theory (eq. (1)).
Comparisons of the experimental c_N with those calculated from equa-
tion (4) are presented in figure 8. In all cases, generally good agree-
ment is obtained between experimental and empirical values of normal-
force coefficient up to angles of attack of about 35°.

Maximum Lift Coefficient

The maximum lift coefficient of each of the wings is presented in
figure 9 as a function of Mach number. Maximum lift coefficient was
obtained as discussed previously by a linear extrapolation of curves of
$c_L/\cos \alpha$ vs. α. The plot includes additional $c_{L_{max}}$ data from refer-
ences 1, 2, 13, and 14 for higher aspect ratio triangular wings. A
relatively large decrease in $c_{L_{max}}$ is indicated when the aspect ratio
is decreased below a value of 2; above 2, only a slight effect of aspect

ratio on $C_{L_{max}}$ is shown. All of the wings show approximately the same
decrease in $C_{L_{max}}$ with increasing Mach number. A simple correlation
of these effects of aspect ratio and Mach number is presented in figure 10
where $C_{L_{max}}$ is plotted as a function of the ratio of Mach number to
aspect ratio. The data of the present tests and of references 1, 2, 13,
and 14 are shown to lie within ±5 percent of an average curve. The curve
drawn gives the approximate result,

$$C_{L_{max}} \approx \frac{1}{(M/A)^{1/6}}$$

CONCLUSIONS

Measurements were made in the Mach number range 1.96 to 3.30 of the
lift and normal force on three triangular wings of aspect ratio 3/8, 2/3,
and 1 at angles of attack up to 47°. An analysis of the results of this
investigation has led to the following conclusions:

1. Near zero angle of attack the normal-force curve slopes are
satisfactorily predicted by linear theory. Above angles of attack of
about 5°, however, available nonlinear theories for low-aspect-ratio
triangular wings are inadequate for predicting the large nonlinearities
in the normal-force curves.

2. Normal-force coefficients can be predicted for angles of attack
up to at least 30° by utilizing linear theory plus a nonlinear empirical
expression for the nonlinear components of normal-force coefficients.

3. Comparisons of the maximum lift coefficients of the present
report with data for larger aspect ratio wings from other investigations
show that effects of aspect ratio become significant only below a value
of about 2. The maximum lift coefficient decreases approximately 30
percent when the aspect ratio is decreased from 2 to 3/8.

4. For wings ranging in aspect ratio from 3/8 to 4, the maximum
lift coefficient decreases with increasing Mach number.

5. Maximum lift coefficient can be correlated to within ±5 percent
when plotted as a function of the ratio of Mach number to aspect ratio.

Ames Aeronautical Laboratory
    National Advisory Committee for Aeronautics
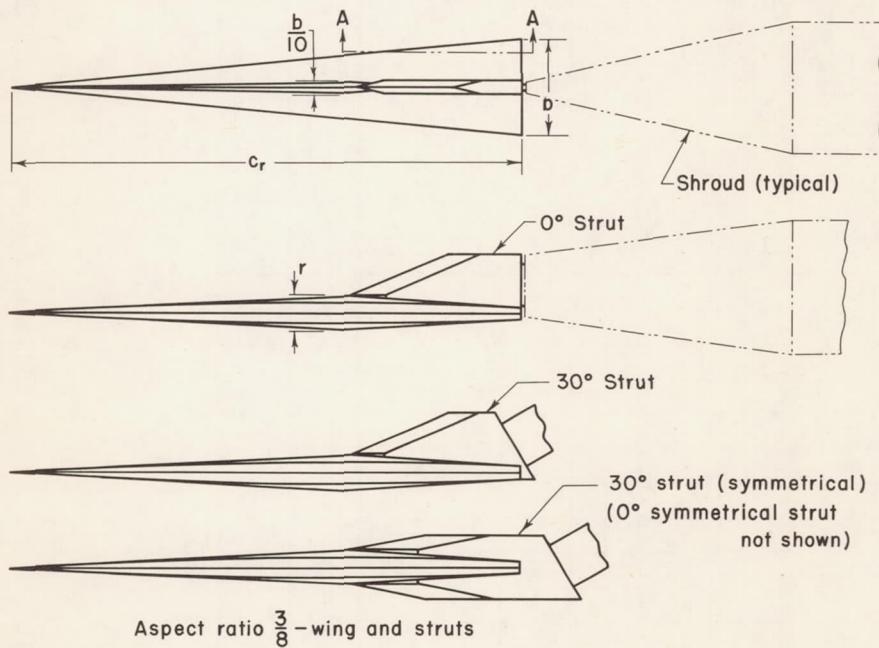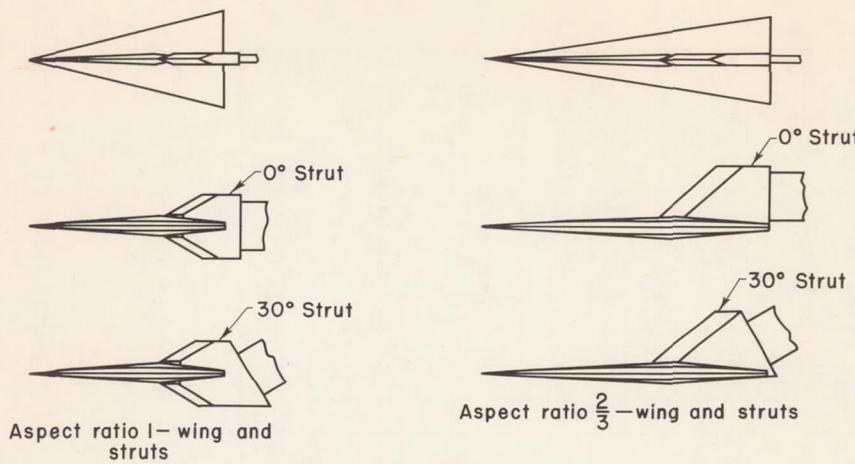   Moffett Field, Calif., Sept. 17, 1957

REFERENCES

1. Kaattari, George E.: Pressure Distributions on Triangular and Rectangular Wings to High Angles of Attack - Mach Numbers 1.45 and 1.97. NACA RM A54D19, 1954.

2. Kaattari, George E.: Pressure Distributions on Triangular and Rectangular Wings to High Angles of Attack - Mach Numbers 2.46 and 3.36. NACA RM A54J12, 1955.

3. Katzen, Elliott D., and Pitts, William C.: Load Distributions on Wings and Wing-Body Combinations at High Angles of Attack and Supersonic Speeds. NACA RM A55E17, 1955.

4. Pitts, William C.: Force, Moment, and Pressure-Distribution Characteristics of Rectangular Wings at High Angles of Attack and Supersonic Speeds. NACA RM A55K09, 1956.

5. Hill, William A., Jr., and Kaattari, George E.: Force and Pressure-Distribution Investigation to High Angles of Attack on All-Movable Triangular and Rectangular Wings in Combination With a Body at Supersonic Speeds. NACA RM A56C12, 1956.

6. Nielsen, Jack N., Spahr, J. Richard, and Centolanzi, Frank: Aerodynamics of Bodies, Wings, and Wing-Body Combinations at High Angles of Attack and Supersonic Speeds. NACA RM A55L13c, 1956.

7. Küchemann, D.: A Non-Linear Lifting-Surface Theory for Wings of Small Aspect Ratio with Edge Separations. RAE Rep. No. Aero. 2540, British, 1955.

8. Edwards, R. H.: Leading-Edge Separation from Delta Wings. Jour. Aero. Sci., Readers Forum, vol. 21, no. 2, Feb. 1954, pp. 134-135.

9. Brown, Clinton E., and Michael, William H., Jr.: On Slender Delta Wings With Leading-Edge Separation. NACA TN 3430, 1955.

10. Jones, Robert T.: Properties of Low-Aspect-Ratio Pointed Wings at Speeds Below and Above the Speed of Sound. NACA Rep. 835, 1946.

11. Stewart, H. J.: Lift of a Delta Wing at Supersonic Speeds. Quart. Appl. Math., vol. 4, no. 3, Oct. 1946, pp. 246-254.

12. Tosti, Louis P.: Low-Speed Static Stability and Damping-in-Roll Characteristics of Some Swept and Unswept Low-Aspect-Ratio Wings. NACA TN 1468, 1947.

13. Smith, Fred M.: Experimental and Theoretical Aerodynamic Characteristics of Two Low-Aspect-Ratio Delta Wings at Angles of Attack to 50° at a Mach Number of 4.07. NACA RM L57E02, 1957.

14. Gallagher, James J., and Mueller, James N.: An Investigation of the Maximum Lift of Wings at Supersonic Speeds. NACA Rep. 1227, 1955. (Supersedes NACA RM L7J10)
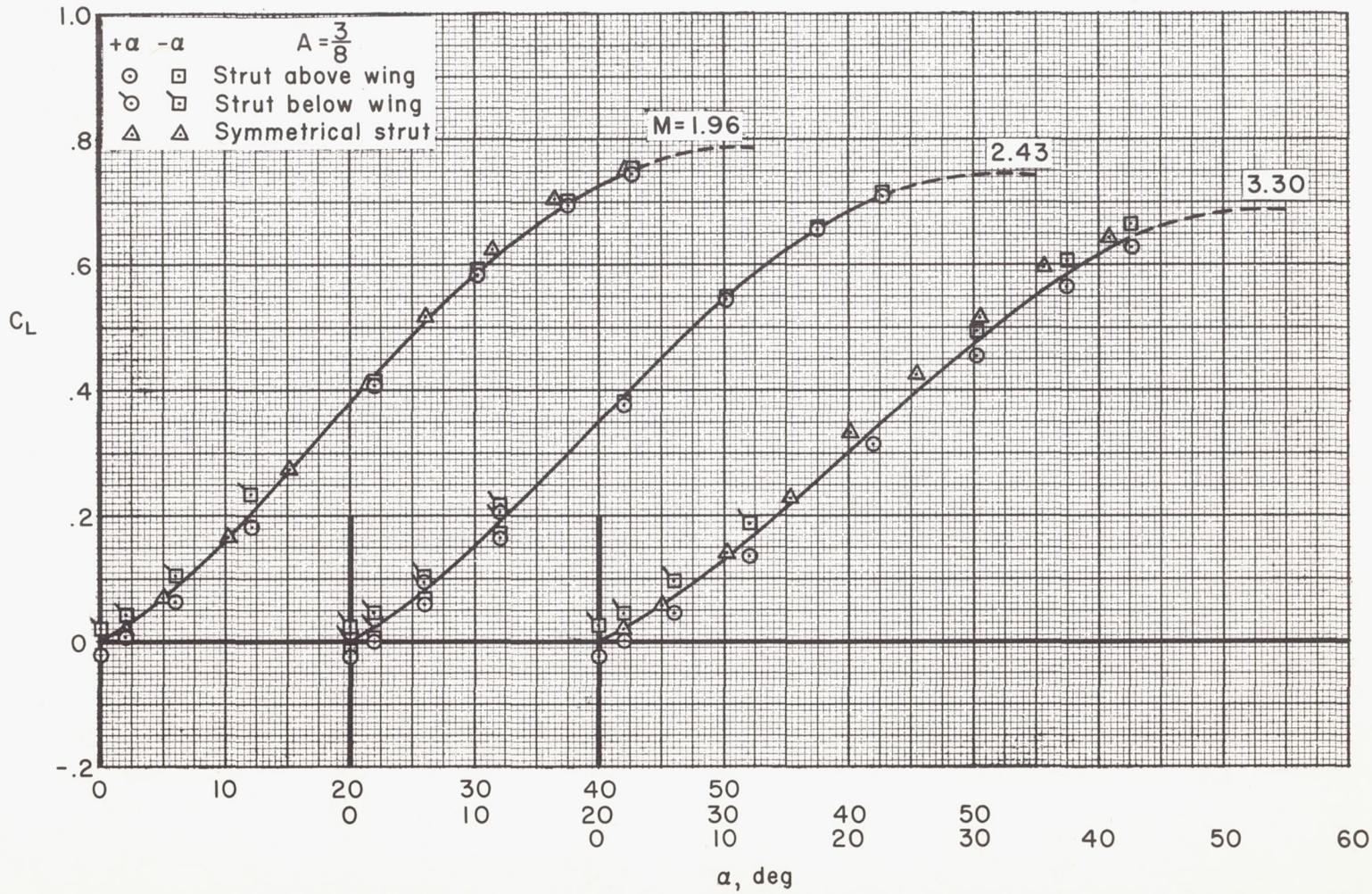
Section A-A (typical) modified biconvex

Shroud (typical)

Aspect ratio 1— wing and struts

Aspect ratio $\frac{2}{3}$ —wing and struts

Aspect ratio $\frac{3}{8}$ —wing and struts

Aspect ratio	b, in.	c_r, in.	Area sq. in.	$\left(\frac{t}{c}\right)_{max}$	r, in.
$\frac{3}{8}$	1.5	8	6.00	0.04	0.50
$\frac{2}{3}$	1.5	4.5	3.37	0.04	0.25
1	1.5	3	2.25	0.04	0.25

Figure 1.- Summary of model geometry and dimensions.

Figure 2.- Variation of lift coefficient with angle of attack for triangular wing of aspect ratio 3/8.
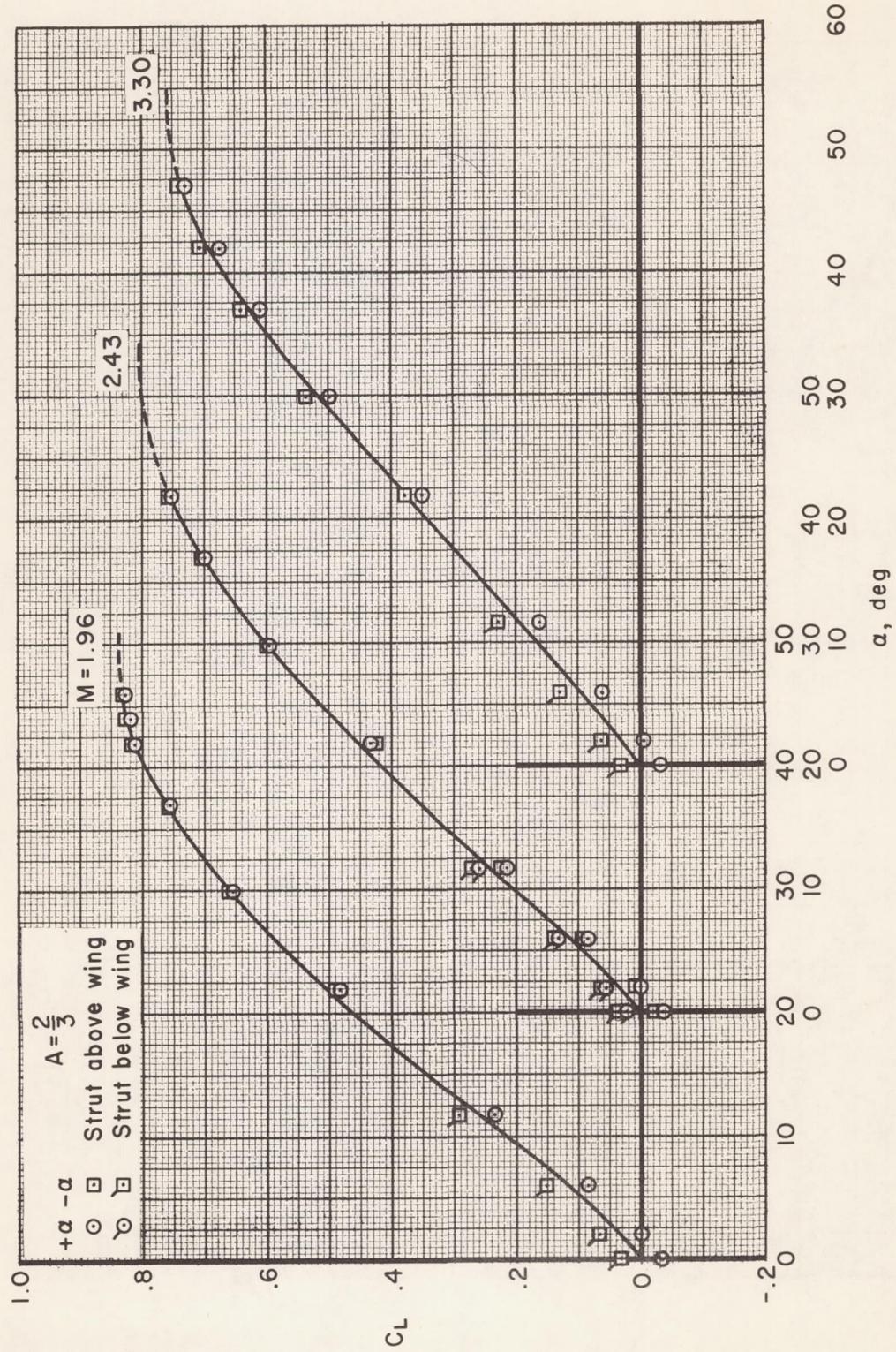
Figure 3.- Variation of lift coefficient with angle of attack for triangular wing of aspect ratio 2/3.
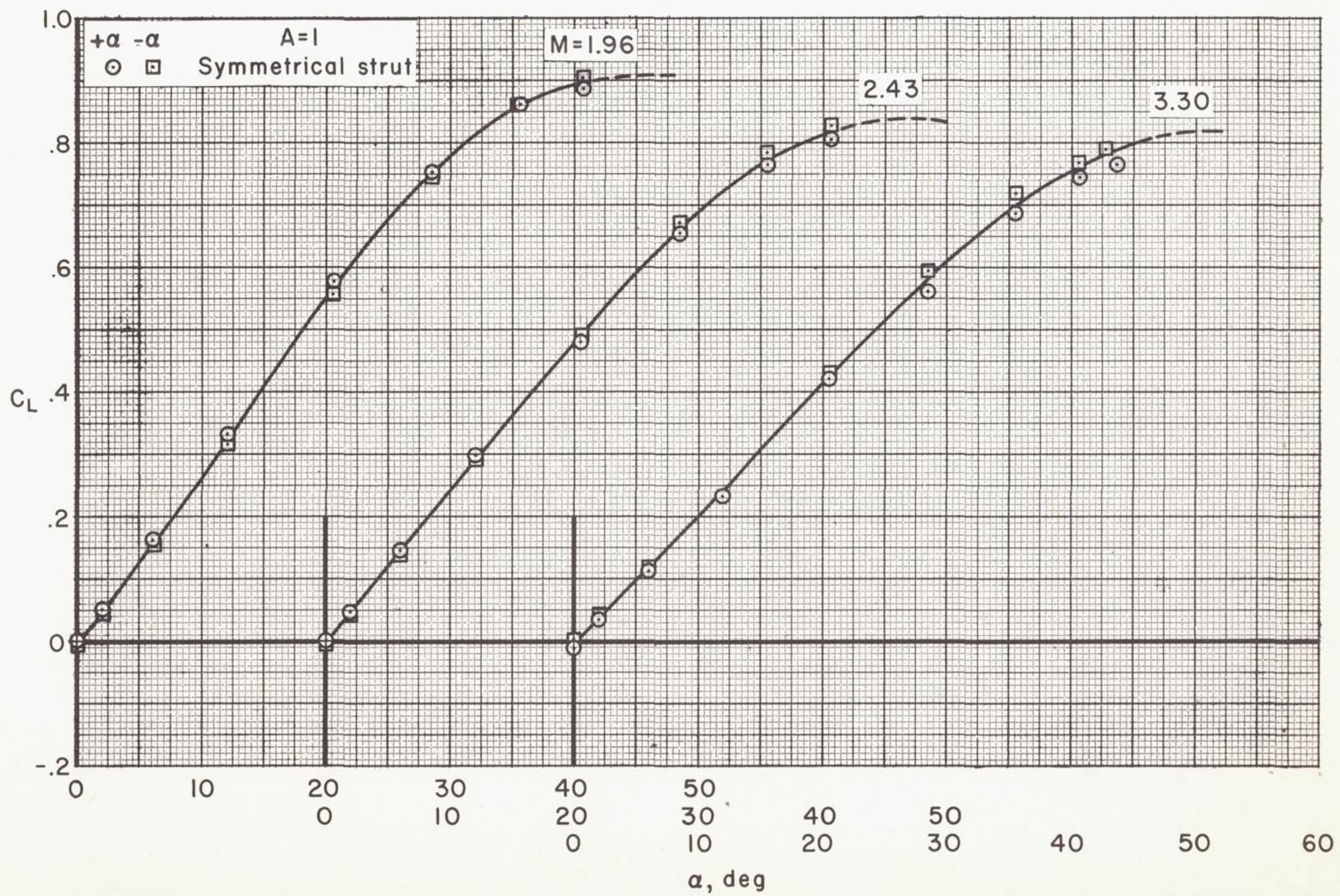
Figure 4.- Variation of lift coefficient with angle of attack for triangular wing of aspect ratio 1.
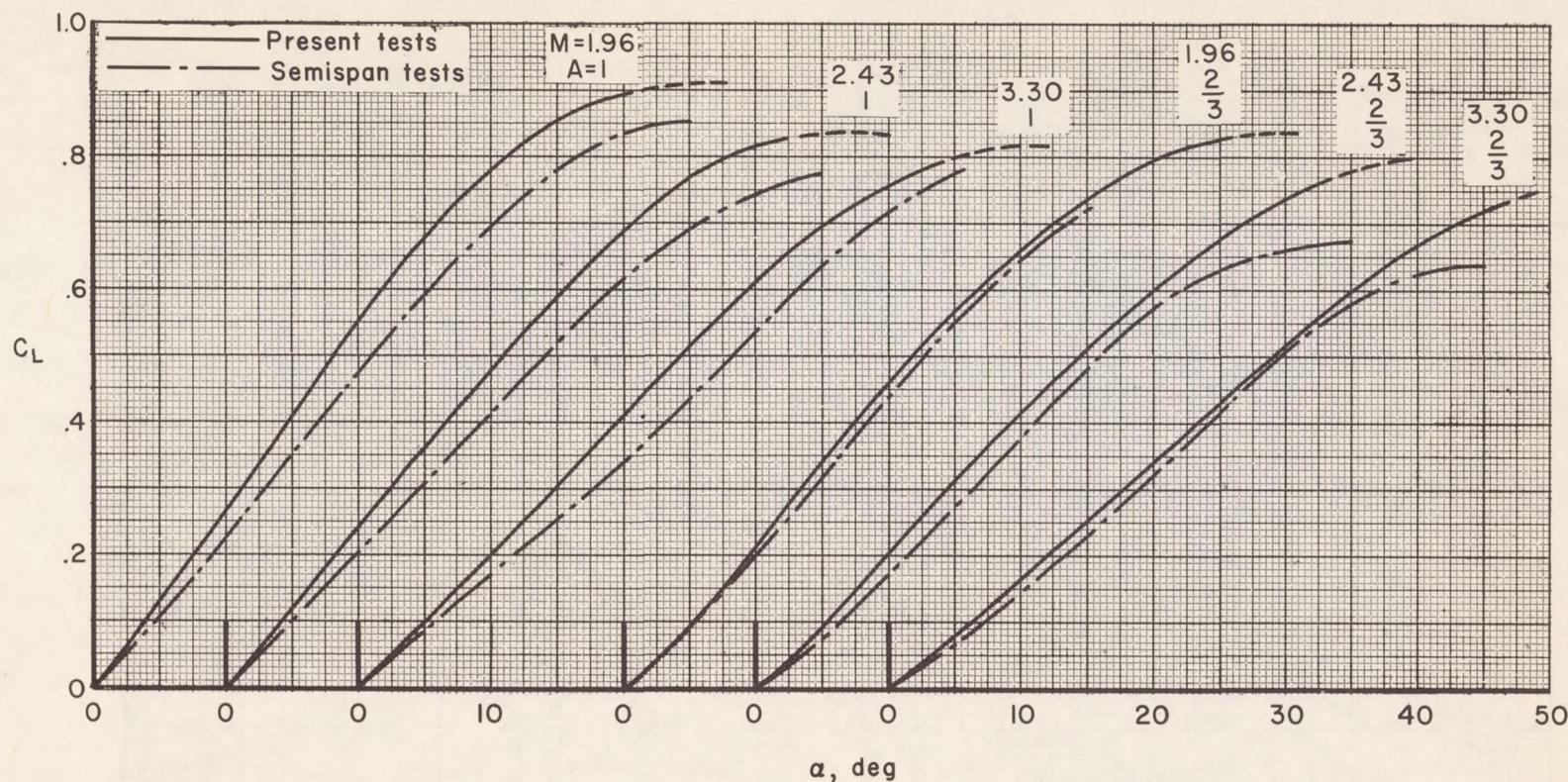
(a) A = 1 and 2/3

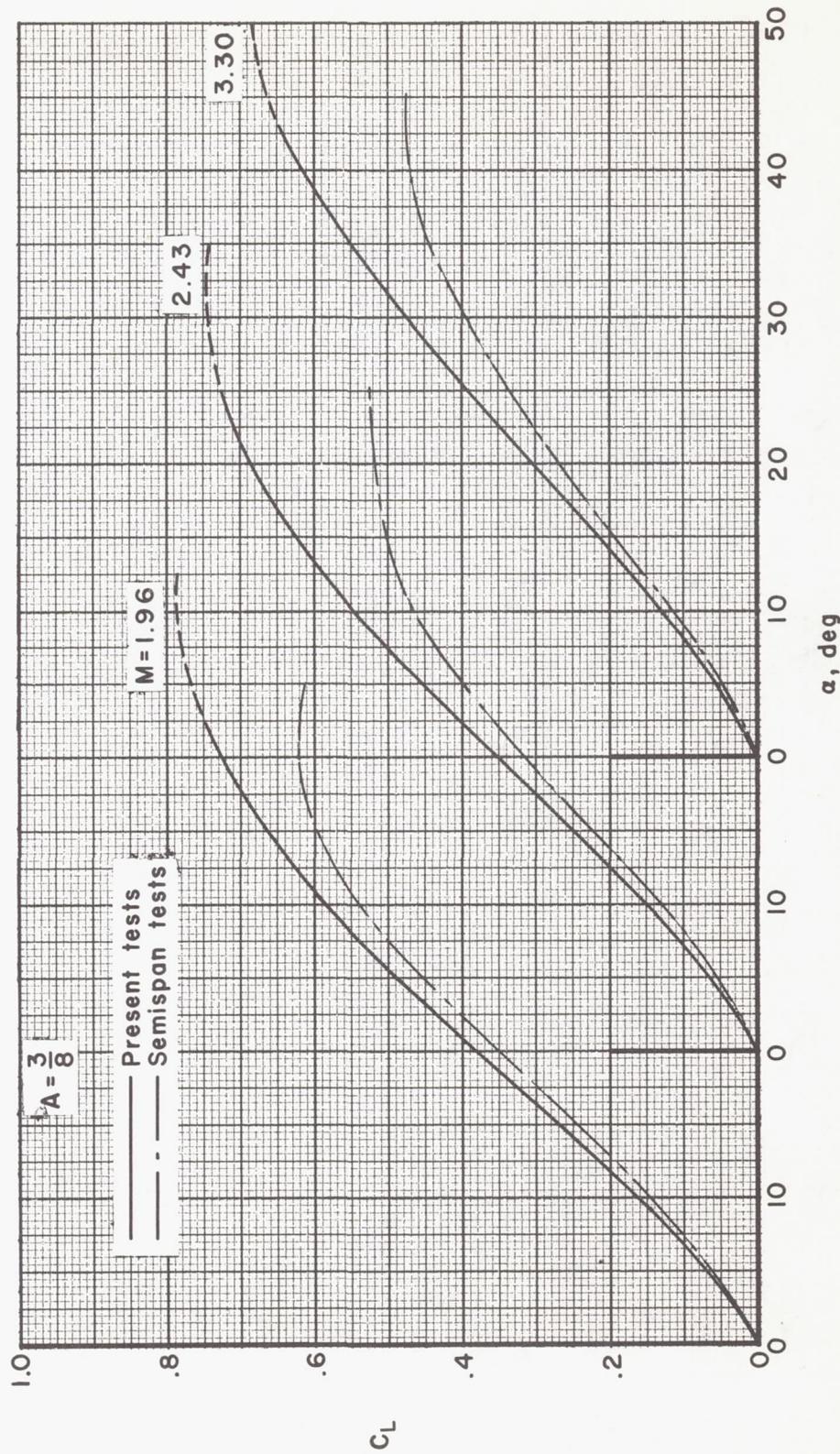Figure 5.- Comparison of the lift curves of similar full-span and semispan triangular wings.
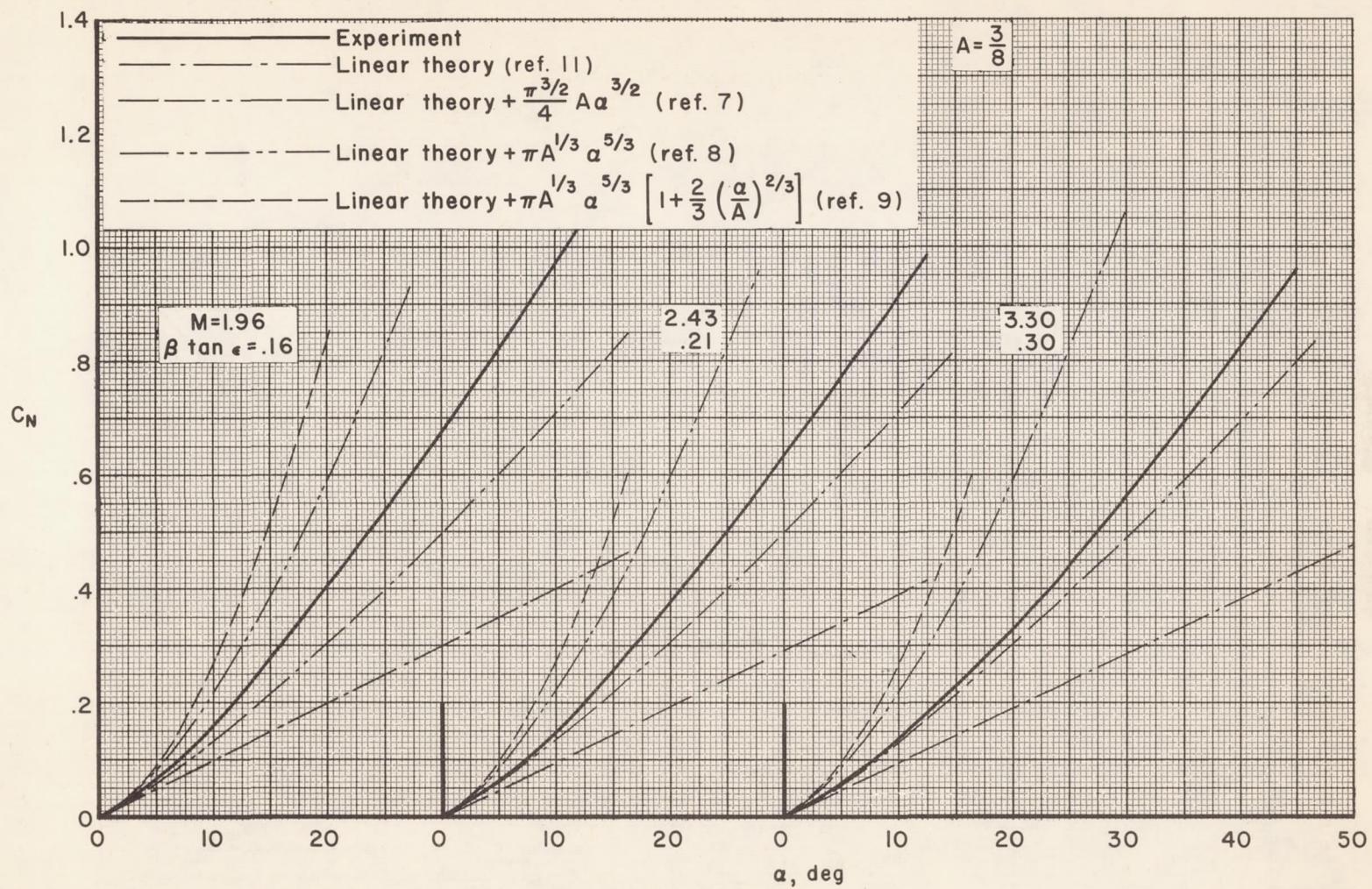
(b) A = 3/8

Figure 5.- Concluded.

(a) A = 3/8

Figure 6.- Comparison of experimental and theoretical values of normal-force coefficient.
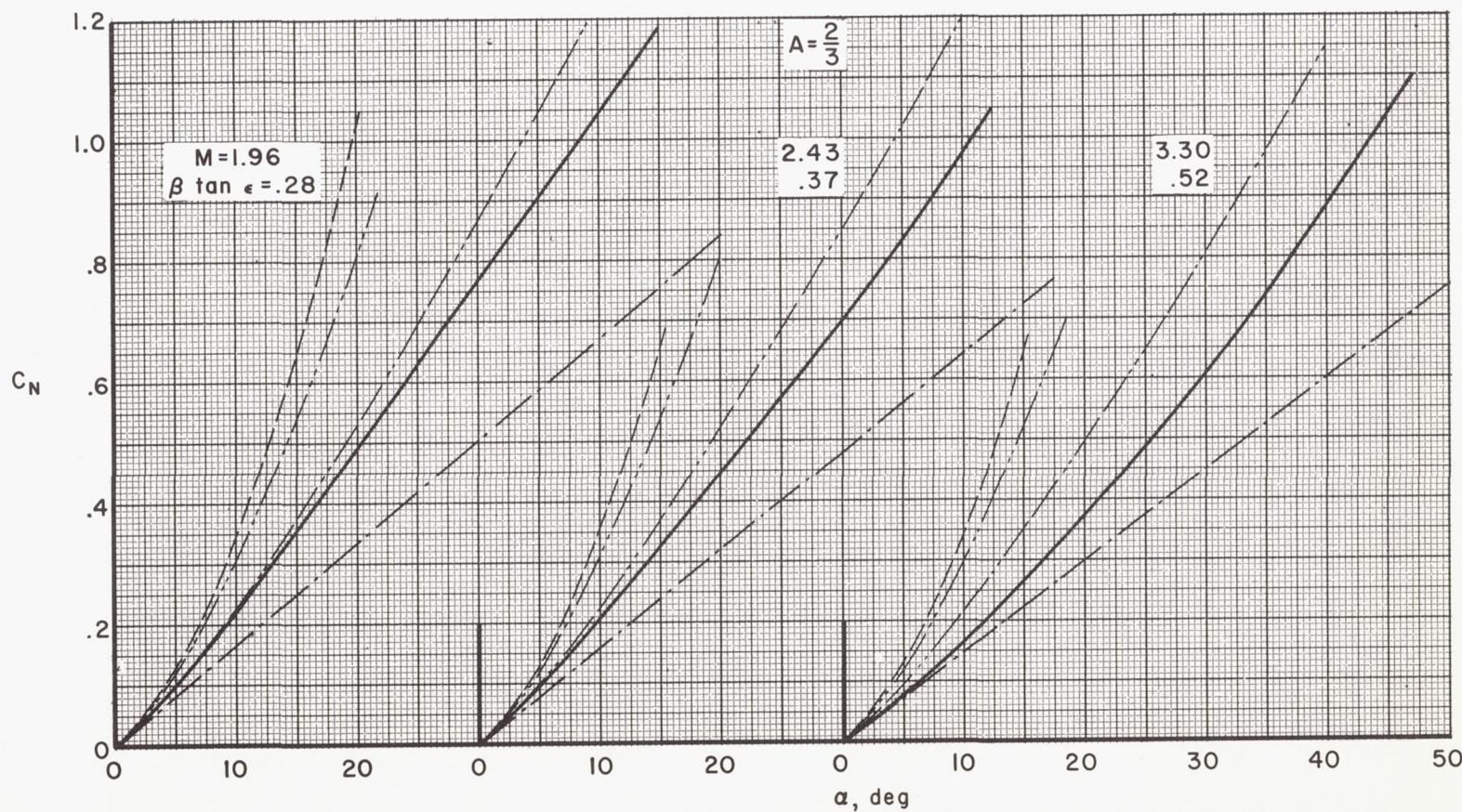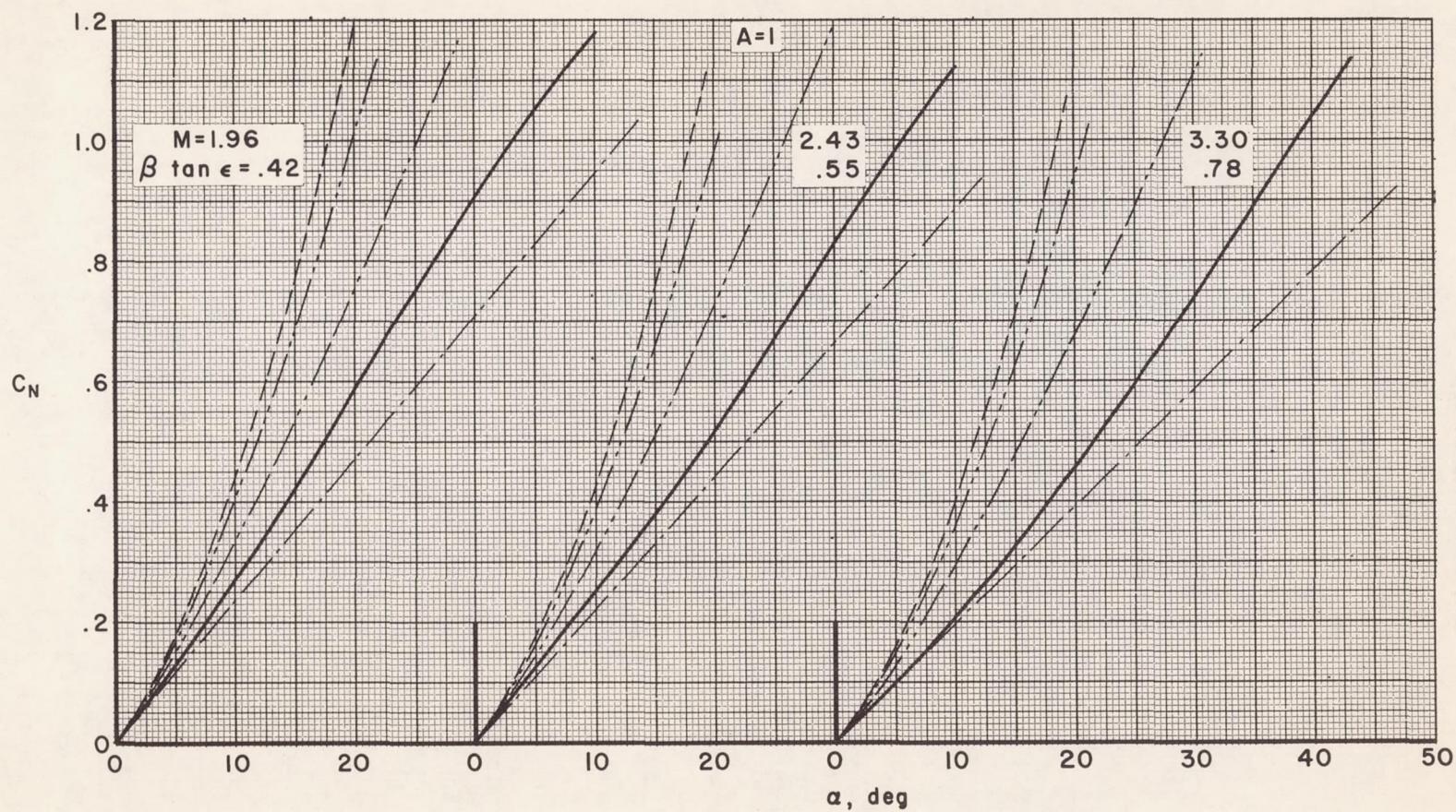
(b) A = 2/3

Figure 6.- Continued.

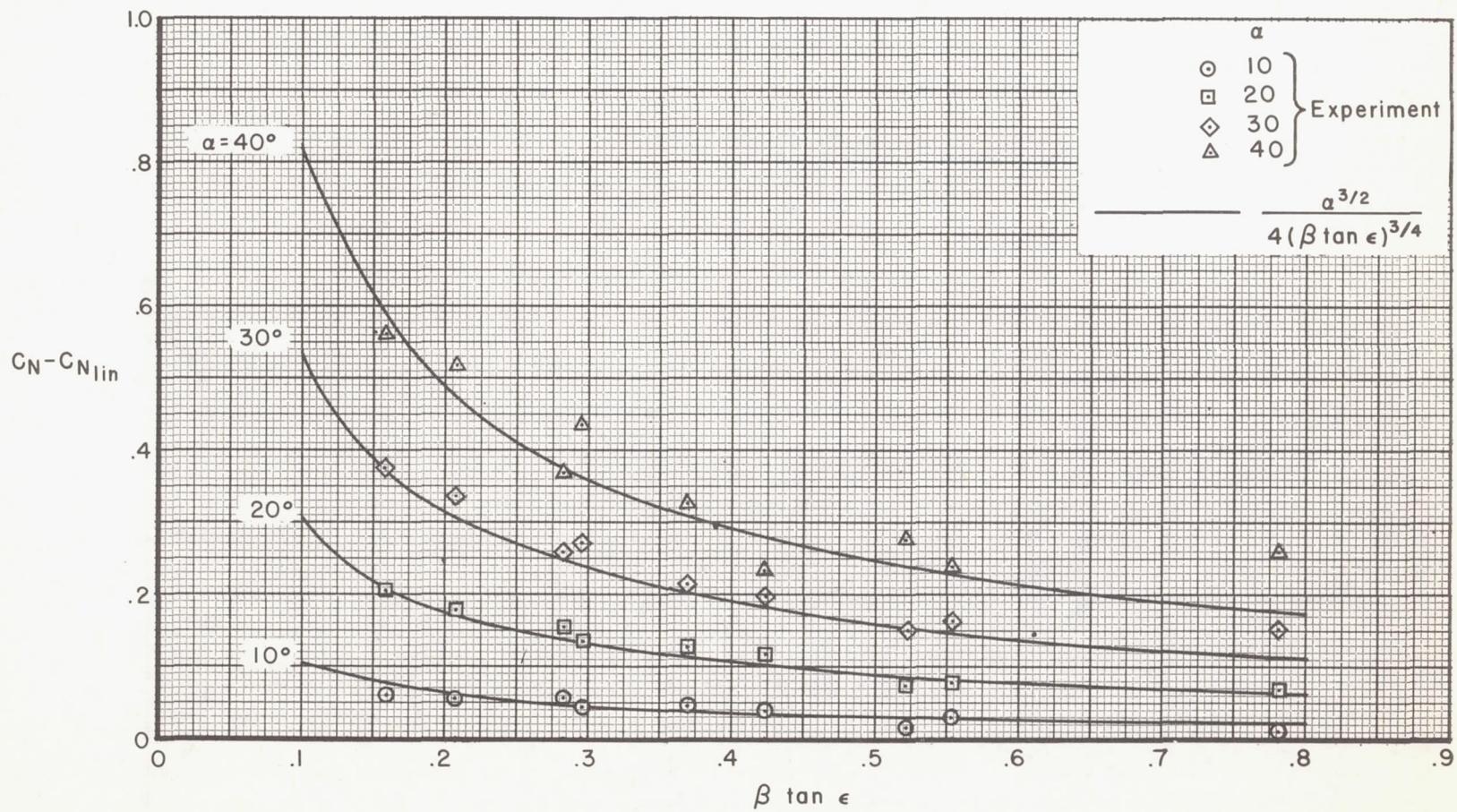(c) A = 1

Figure 6.- Concluded.

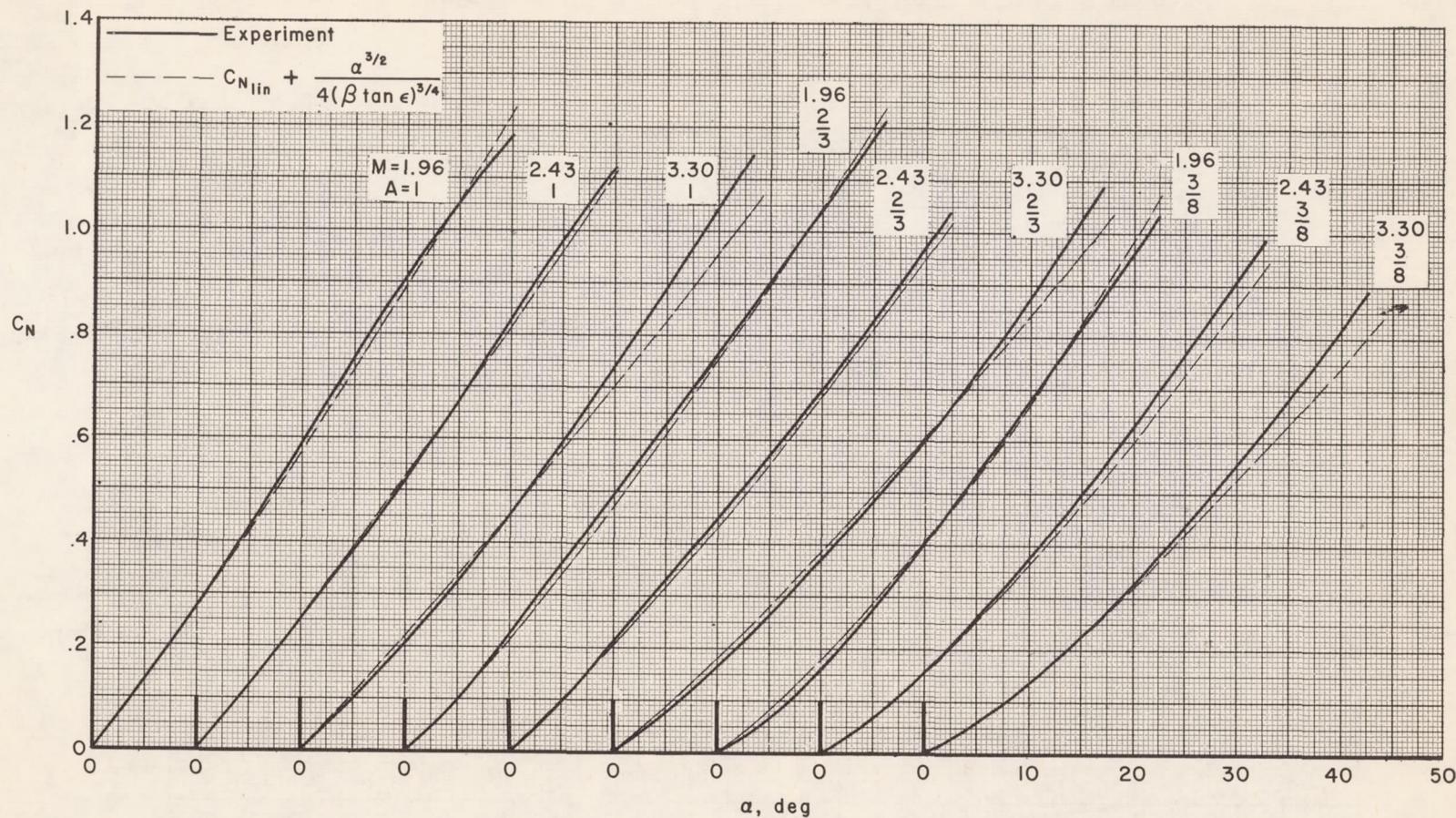Figure 7.- Correlation of nonlinear component of normal-force coefficient with $\beta \tan \epsilon$.

Figure 8.- Comparison of experimental and empirically predicted values of normal-force coefficient.

1.2

1.0

.8

$C_{L_{max}}$

.6

.4

.2

0

1.0   1.4   1.8   2.2   2.6   3.0   3.4   3.8   4.2

M

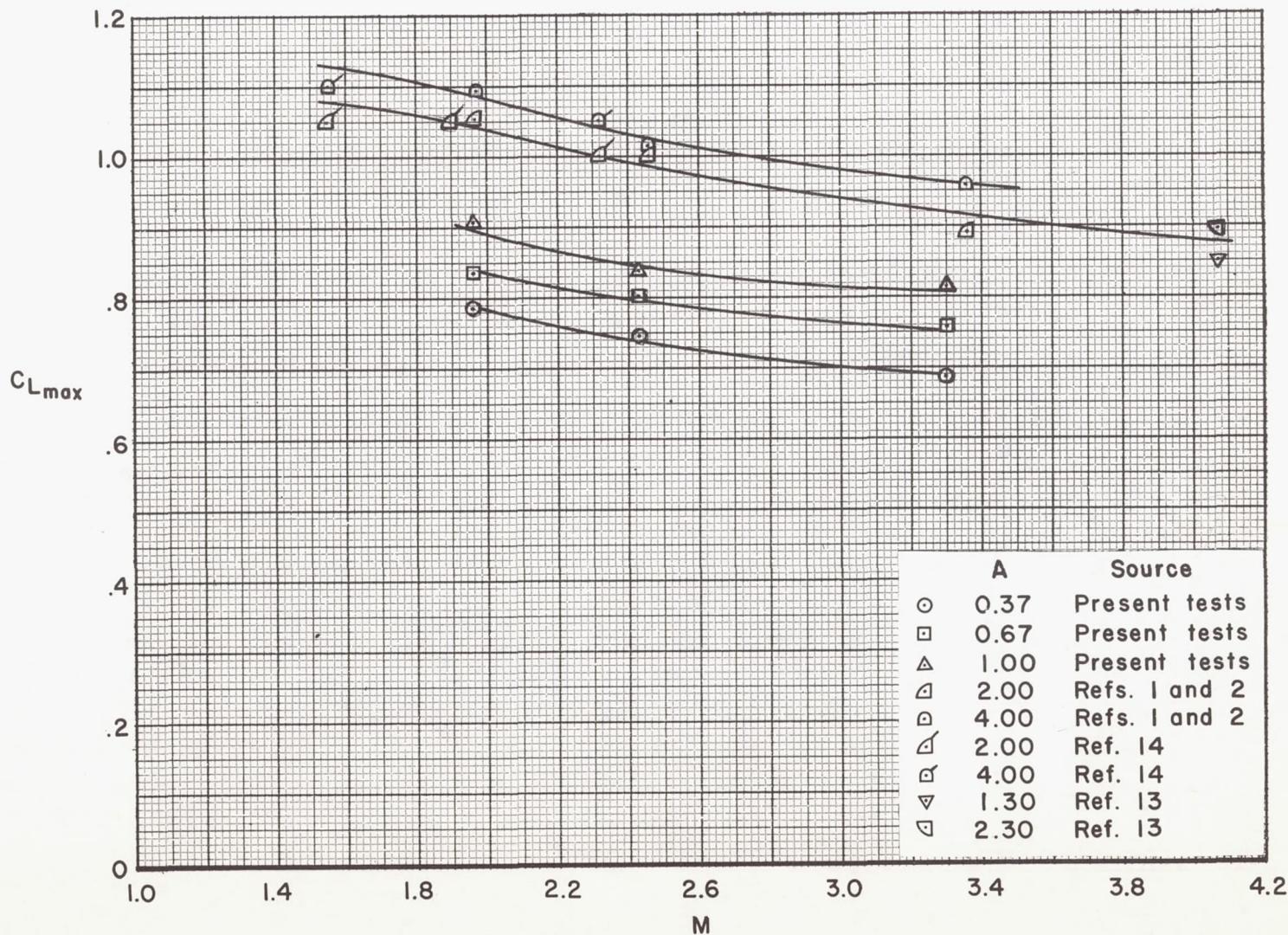|	A	Source
⊙	0.37	Present tests
⊡	0.67	Present tests
△	1.00	Present tests
◁	2.00	Refs. 1 and 2
◠	4.00	Refs. 1 and 2
◢	2.00	Ref. 14
◰	4.00	Ref. 14
▽	1.30	Ref. 13
◁	2.30	Ref. 13

Figure 9.- Variation of maximum lift coefficient with Mach number.
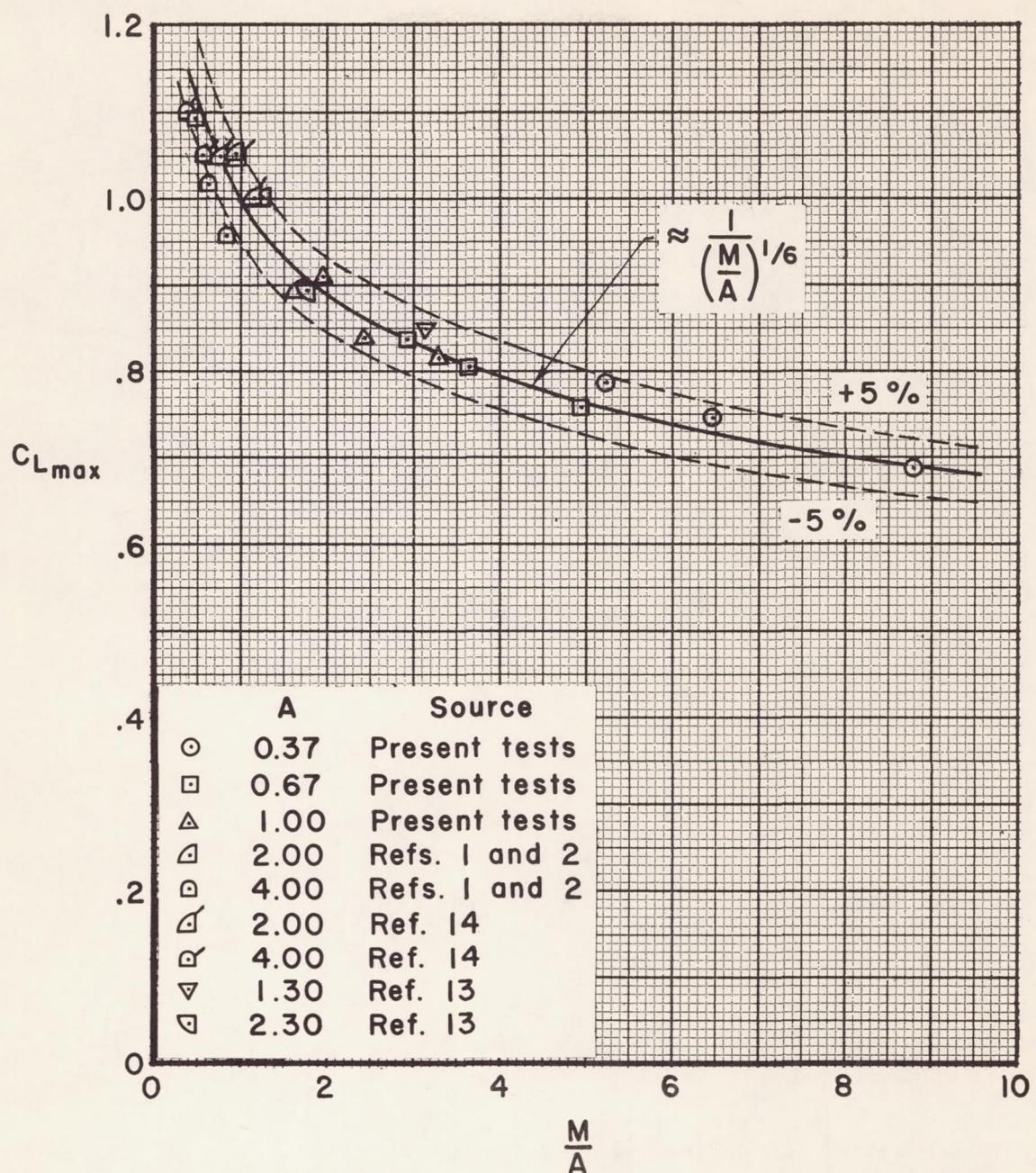
Figure 10.- Correlation of maximum lift coefficient with the ratio of
Mach number to aspect ratio.